Failure Assessment of Steel-Concrete Composite Column Under Blast Loading

Marcin P. BUDZIAK, Tomasz GARBOWSKI

Poznan University of Technology
Institute of Structural Engineering
Piotrowo 5, 60-965 Poznań, Poland
e-mail: tomasz.garbowski@put.poznan.pl

Composite column as a key structural member can be subjected to a blast load as a result of an accident or a terrorist threat. In this paper, a method for assessing the blast resistance of a composite concrete-filled column is proposed. Moreover, different methods of enhancing composite member resistance to explosions are investigated. The blast situation is modeled in the FEM software using the CONWEP tool. This empirical formulation is relatively cheap from the computational point of view, as well as precise enough, hence it was chosen for this work purposes. Material models are based on well known elasto-plastic with linear hardening concepts. Important phenomenons are also taken into account, such as: contact formulation between the column components, strain rate dependence, damage initiation and evolution. Simulations are conducted for the most common type of explosion – surface blast. Its main feature is the effect of reflection of the ground surface and hence, amplification of the blast wave after the charge ignition. Results are presented in terms of minimum TNT mass equivalent required for a column member failure.

Key words: composite column, blast loading, failure assessment.

1. INTRODUCTION

Designing a building is a process where many goals such as functionality, aesthetic appearance, durability, bearing capacity have to be achieved. However, the most important thing is to provide safety to the users. Recent years show, that structural engineers have to bring more attention to accidental loading, from which explosions seem to be the most dangerous, as they can significantly damage the structure or even cause its total failure. The most fateful cases such as World Trade Center collapse on 11th September 2001 [21] are very well described explaining specific causes and effects. Hence, possible acts of terrorism have to be taken into consideration all over the world, at the earliest buildings' life phase during the design procedure. Also industrial buildings, where

explosion risk exists due to explosive materials production or storage, should be investigated for resistance to such events. In the literature a lot of examples may be found to prove the necessity of assessment the structural response of a building in a blast situation.

Apart from the structure strength some phenomena should not be neglected. First, the difference has to be studied between detonation of charge in the air and on the ground surface. The second situation is much more common and unfortunately much more destructive. What is more complex, the enhancement of damage depends on the type of ground. The more energy is dissipated in producing a crater and groundshock, the less damage to the structure may be observed. Another important issue is the "tunneling" effect in narrow city streets [22]. Low distance between buildings results in confinement of the blast wave. It is reflected and refracted repeatedly of the facades' surfaces, hence the damages occur higher than might be expected in open air conditions. Either the glazing type of facades has its impact on the blast wave [23]. The shockwave front penetrates through the openings and people are subjected to sudden pressures and shattered particles of windows, doors, etc. If the external walls are not able to resist the pressure peak they are fractured and moved by the wave following the shock front causing much more serious damages.

Since aforementioned external conditions would distort this investigation results, a separated fragment of the structure will be studied. A column member can be fairly considered as a critical point of the building, hence it was chosen as a subject of the simulations. Empirical tests of explosions are very expensive and time consuming, what results in quite low accessibility of such experiments in civil engineering field [24]. Fortunately, it is feasible, to conduct numerical simulations at relatively low cost of both an explosion taking place in given space and time, as well as the structure response to such action. Moreover, there exist a need to provide to structural designers a reliable tools for assessing structure resistance in terms of blast situation.

Any realistic simulation of a blast effect on the structure requires suitable constitutive models of structural materials as steel, concrete, glass, etc. Material models characterized by a standard and/or new testing methods in quasi-static conditions (see e.g. [8, 9]) are applicable only in specific range of strain rates. Popular material models of concrete, e.g. Drucker-Prager [7], Lubliner [19], Lee-Fenves [18] can be successfully used in quasi static elasto-plastic-damage analysis (see e.g. [10, 20]), however, they require slight modifications if one wants to use them in dynamic analyzes. The same concerns traditional material model of steel, e.g. Huber-Mises-Hencky, Johnson-Cook [26] or Gurson [13]. Once constitutive models are enhanced by additional features as damage evolution or fracturing in high strain rates the sophisticated test has to be performed (e.g. Split Hopkinson Pressure Bar test also known as Kolsky bar test

[11, 25]) for material characterization and hence more parameters need to be involved in computations. These new parameters, ensuring they are properly identified, lead to realistic computer simulations of the structure subjected to impact loads.

In this work authors employed available in literature simplified modeling of blast phenomenon as well as traditional constitutive models of structural elements enhanced by damage definition and strain rate dependency. The main goal is to predict the failure mechanism and provide possible reinforcing methods of critical elements of a public buildings structure.

2. Blast model

By definition, an explosion is a rapid release of big amount of energy. It is accompanied by a blast wave which is heat and pressure wave propagation in space. The latter is subject to many research and investigation as its outcome causes the most serious consequences to structures. The blast produces a shock wave composed of a high-intensity shock front which expands outward from the surface of the explosive into the surrounding air. Pressure immediately behind the detonation front is in range from 19,000 MPa to 33,800 MPa (Unified Facilities Criteria 3-340-02, December 2008). Only about one-third of the total chemical energy available in most high explosives is released in the detonation process. The remaining two-thirds are released more slowly in explosions in air as the detonation products mix with air and burn. This afterburning process has only a slight effect on blast wave properties, because it is much slower than detonation.

Throughout the pressure-time profile (Fig. 1), two main phases can be observed – portion above ambient is called positive phase duration, whereas that below ambient is called negative phase duration. The negative phase is of a longer duration and a lower intensity than the positive duration. The shock wave overpressure curve is important from the standpoint of civil engineer as it a basis for determination of dynamic pressure. The dynamic pressure determines the value of loading that is subjecting the structure. Generally blast loading on a structure caused by a high-explosive detonation is dependent upon several factors:

- the magnitude of the explosion,
- the location of the explosion relative to the structure of interest (confined or unconfined),
- the geometrical configuration of the structure,
- the structure orientation with respect to the explosion and the ground surface (above, flush with, or below the ground).
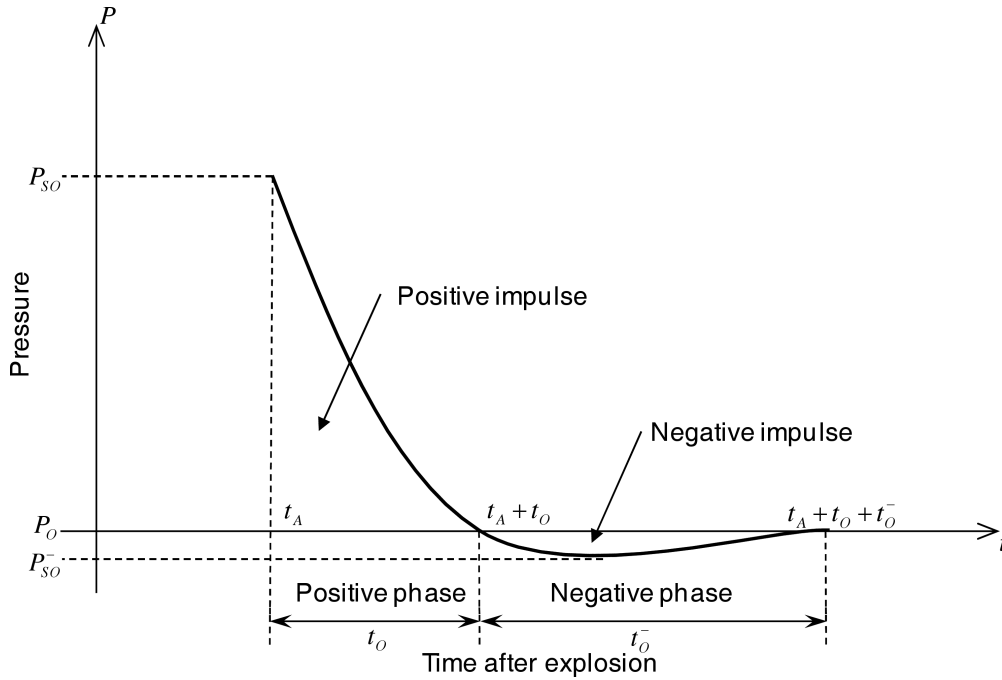
FIG. 1. Relation between time and shock wave pressure.

2.1. Blast-loading classification

Two blast-loading categories can be distinguished. The division bases on the confinement of the explosive charge, and so there are unconfined and confined explosions. For this purposes only two most representative and commonly encountered in practice types of unconfined explosions are presented.

First is called Air Blast and applies to events, where the charge is detonated in free air, enabling unconstrained blast wave propagation.

The second type is known as Surface Blast, which refers to the situation where source of the shock wave is located close to, or on the ground surface. The initial wave of the explosion is reflected and reinforced by the ground surface to produce a reflected wave. Unlike the air burst, the reflected wave merges with the incident wave at the point of detonation to form a single wave, similar in nature to the Mach wave of the air burst but essentially hemispherical in shape.

2.2. Numerical model of blast event

The most considered effect of an explosion is blast overpressure wave. Various methods of estimating the blast peak overpressure based on empirical formulas

were collected in literature [3, 23], however all they base on a scaled distance, which is denoted as:

$$Z = \frac{R}{W^{1/3}},$$ (2.1)

where R is distance to the charge and W is mass of the charge given in kg of TNT.

Numerical methods of analyzing explosion problems and blast-loading modeling can be divided into two stages. First, modeling of the shock wave. Second, formulation of the interaction with a structure subjected to such load. Blast wave modeling requires the determination of the charge weight given in TNT-equivalent and charge localization coordinates. Also type of the explosion has to be selected as the air or surface blast. Output data returns a pressure in given space point, occurring at a given time.

One of the most commonly used numerical tool for blast modeling is Con-Wep. It is mathematical model based on empirical data of experimental detonations of explosives of masses from less than 1 kg to over 400 000 kg [17]. This data was then scaled using Hopkinson and Sachs scaling laws to standard atmospheric sea level conditions. Formulas prepared by Kingery and Bulmash [17] allow estimating shock wave parameters basing on TNT only. For other explosives TNT-equivalent has to be used accordingly to its type. Once the parameters of peak overpressure, time of arrival and time of duration are determined, the value of the pressure in time is given by the modified Friedlander's Equation proposed in [3]:

$$p = P_s \left(1 - \frac{t - t_a}{t_s}\right) e^{-b(t-t_a)/t_s},$$ (2.2)

where P_s is the peak overpressure, t_a is the time of arrival, t_s is the positive phase duration for the overpressure, and b denotes the decay coefficient.

The main advantage of this model is that the loading is applied directly to the structure subjected to the blast. There is no need to include the fluid medium in the computational domain. Since the considered time of blast is relatively short, this model seems to be good approximation of the pressures applied to the investigated surface. However, It does not account for the effects of the soil over a buried bomb or the pressure wave that travels through the surrounding air. Moreover, it does not take into account the wave reflection effects. These drawbacks cause ConWep to underestimate damage and deformation. An alternative to ConWep is the Arbitrary Lagrangian Eulerian method (ALE), which can simulate the compound effects of pressure, air, and soil [27]. While it is a more realistic modeling method, it is vastly more complex and costly and not a feasible option for the scale of this investigation. Figures below

(Fig. 2, Fig. 3) present research comparing experimental results and ConWep estimations. ConWep estimations show excellent agreement with experimental results. Since the scale of tested events in this paper is similar, ConWep is con-
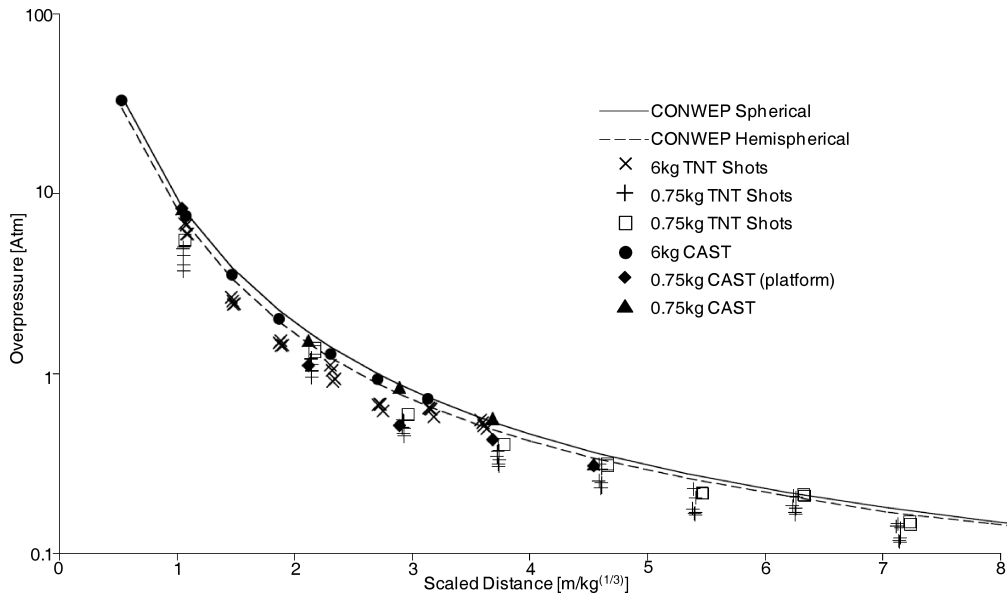

FIG. 2. Peak overpressure and shock arrival time in relation to scaled distance [16].
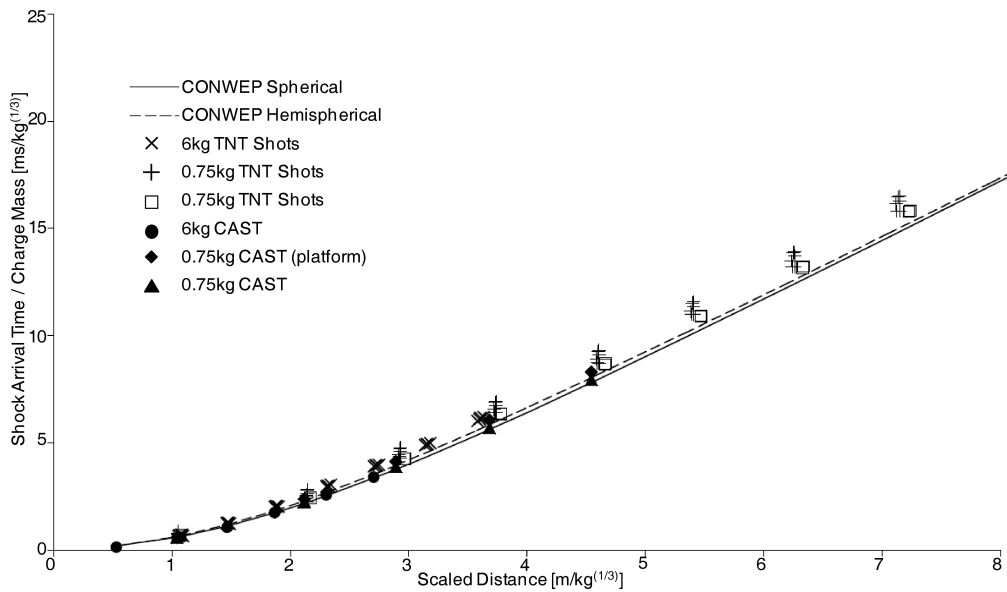

FIG. 3. Shock arrival time in relation to scaled distance [16].

sidered a very good tool for numerical modeling of the blast wave for this work purposes.

3. Material model

Steel and concrete investigated in the composite column require different material models to reflect their structural behavior both in static and dynamic load case. Concepts presented below provide simulation of material response to actions.

3.1. Steel

For both, structural and reinforcing steel the elasto-plastic model with linear hardening was employed. Essential matter is the yield criterion choice. Among many sophisticated concepts, that are available for FEM application, well proven Huber-Mises-Hencky (HMH) yield criterion was used. The HMH criterion is based on a definition of effective stress computed solely on the second deviatoric stress invariant:

$$(3.1) \qquad \overline{\sigma} = \sqrt{3J_2}.$$

The yield surface function may be presented graphically, as an infinitely long cylinder with geometric axis covering the zero hydrostatic stress axis in the principal stress space for agreed value of the hardening value. Application of equivalent stress and associated equivalent plastic strain, as internal variable of the hardening function, derives the plastic load function in the form:

$$(3.2) \qquad f = \overline{\sigma}\left(J_2\right) - H\left(\overline{\varepsilon}^{\mathrm{pl}}\right),$$

where $\overline{\sigma}$ is an equivalent stress, also known as q; H denotes the hardening function (related to effective plastic strain) describing the yield surface.

3.2. Concrete

Commonly used concrete in civil structures presents tensile strength approximately ten times lower than compressive strength. Subjected to excessive tension undergoes brittle fracture. As a result of this aforementioned HMH criterion is no longer applicable. Therefore the Drucker-Prager yield criterion [7] was used to describe concrete yield surface. It was derived as a smooth approximation of the Mohr-Coulomb Law. It consists of a modified HMH criterion, in which additional component is introduced defining pressure dependence. According to Drucker-Prager criterion, yield stress occurs when the effective stress q and hydrostatic stresses p reach their critical combination.

The linear Drucker-Prager model (Fig. 4) is used herein. It is written in terms of all three stress invariants and enables the possibility of obtaining noncircular yield surface in the deviatoric plane. In general the criterion is denoted:

$$(3.3) \qquad F = t - p \tan \beta - d = 0,$$

where d is the cohesion of the material, β is the friction angle and t is the modified effective stress. In particular, when t is equal to the equivalent stress q the yield surface is the HMH circle in the deviatoric principal stress plane. The plastic flow is described by the flow rule [7] in the form:

$$(3.4) \qquad G = t - p \tan \psi,$$

where ψ is the dilation angle, which impacts the hardening function. Herein the nonassociated flow in the $p-t$ plane is expected. If $0 \leq \psi < \beta$ the material dilates.
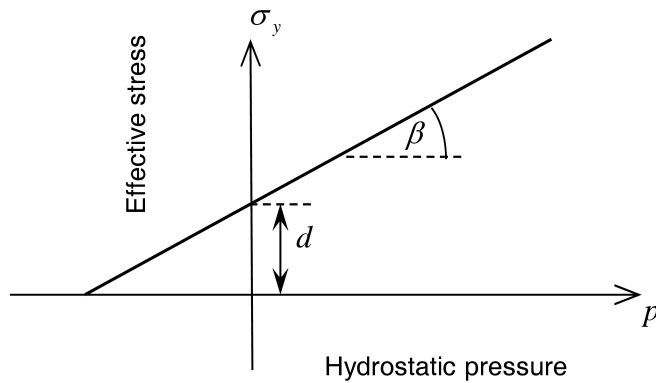

Fig. 4. Linear Drucker-Prager model in meridional plane.

4. STRAIN RATE DEPENDENCE

Material constitutive relationships vary according to the rate of loading applied to the structure. It is necessary to foresee all types of loadings (Fig. 5), that are likely to be encountered during the design lifetime. Material behavior can be affected by the loading rate but, in most cases the difference only becomes
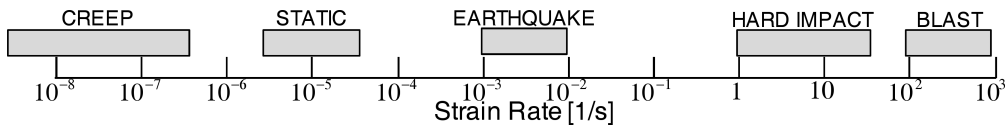

Fig. 5. Magintude of strain rates expected for different loading cases.

significant when the rate changes by more than one order of magnitude [2]. Since the blast situation is considered in this paper, strain rate dependency should not be neglected.

Many experiments proved, that materials such as concrete and steel show strength increase when the strain velocity increases. It can be noticed, that the yield limit growth is significant according to strain velocity raise, however the limit strain decreases respectively. Many methods of implementing this phenomenon to constitutive relations have been developed [14]. In general the problem may be noted in the form:

$$(4.1) \qquad s = \sigma_0\left(\overline{\varepsilon}^{\mathrm{pl}}, \theta\right) R\left(\overline{\varepsilon}^{\mathrm{pl}}, \theta\right),$$

where s is the yield stress including the strain rate dependence, σ_0 is the static yield stress and R is the nonzero strain rate stress to static stress ratio, both function of equivalent plastic strain $\left(\overline{\varepsilon}^{\mathrm{pl}}\right)$ and temperature (θ).

Standard power law of Cowper-Symonds' [5] was used for the R parameter derivation:

$$(4.2) \qquad \dot{\overline{\varepsilon}}^{\mathrm{pl}} = M(R-1)^n,$$

where $M(\theta)$ and $n(\theta)$ are temperature-dependent material parameters.

5. Damage initiation and evolution

Damage in the context of an elastic-plastic material with isotropic hardening is observed in two physical phenomena: softening of the yield stress and degradation of the elasticity. Two main mechanisms can cause the fracture of a ductile metal: ductile fracture due to the nucleation, growth, and coalescence of voids; and shear fracture due to shear band localization. Based on phenomenological observations, these two mechanisms call for different forms of the criteria.

The ductile criterion is a phenomenological model for predicting the onset of damage due to nucleation, growth, and coalescence of voids. The model assumes that the equivalent plastic strain at the onset of damage, $\overline{\varepsilon}_D^{\mathrm{pl}}$, is a function of stress triaxiality $\eta = -p/q$ and strain rate $\dot{\overline{\varepsilon}}^{\mathrm{pl}}$, where p is the pressure stress and q is the equivalent stress. The criterion for damage initiation is met when the following condition is satisfied:

$$(5.1) \qquad \omega_D = \int \frac{d\overline{\varepsilon}^{\mathrm{pl}}}{\overline{\varepsilon}_D^{\mathrm{pl}}\left(\eta, \dot{\overline{\varepsilon}}^{\mathrm{pl}}\right)} = 1,$$

where ω_D is a state variable that increases monotonically with plastic deformation. At each increment during the analysis the incremental increase in ω_D is computed as:

$$(5.2) \qquad \Delta\omega_D = \frac{\Delta\varepsilon^{\text{pl}}}{\overline{\varepsilon}_D^{\text{pl}}\left(\eta, \dot{\overline{\varepsilon}}^{\text{pl}}\right)} \geq 0.$$

When the material exhibits strain-softening behavior, leading to strain localization, formulation in terms of stress-strain relations results in a strong mesh dependency of the FEM results. In particular, the dissipated energy decreases with the mesh size. Some mitigation of this undesirable effect is achieved in analysis introducing a characteristic length to the formulation [1, 15]. Since the softening part of the constitutive law is expressed as a stress-displacement relation, the energy dissipated during the damage process is specified per unit area, not per unit volume. This energy is treated as an additional material parameter, and it is used to compute the displacement at which full material damage occurs. This is consistent with the concept of critical energy release rate as a material parameter for fracture mechanics. This formulation ensures that the correct amount of energy is dissipated and greatly alleviates the mesh dependency.

6. Column static design

Subject of this investigation is a composite column made of circular, steel hollow section filled with reinforced concrete, which is presented in the Fig. 6. Columns are considered the most critical members for public buildings such as multi-storey car parking or an airport. Therefore in this paper a column is isolated from its primary structure and tested under assumed boundary and load conditions. The static design of such member was conducted based on the Ultimate Limit State approach recommended in the European code for steel-concrete composite structures design – Eurocode 4. As an arbitrary decision input parameters such as: materials classes, axial load, eccentricity value, column height, boundary conditions where agreed. Since the composite column static design bases on a few independent variables (e.g. steel section radius, thickness, reinforcement ratio, rebars number) there exists more than one feasible solution. Therefore, an algorithm using Matlab scripting software [28] was developed for this purpose. At first, a set of member configurations that fulfill Eurocode 4 requirements is found. Then, optimal arrangement is chosen. The decisive factor in this simple optimization is the minimum structural steel mass. This is justified by the fact, that in this sort of structural member, steel section is considered the most expensive part.

F<small>IG</small>. 6. Model of the reference column.

The input data for column static design are given in Table 1. Bending moment at the column head was applied in the form of eccentricity of the axial compressive force N_{Ed}. For the buckling problem analysis it is assumed, that the effective length of the column is equal to its model length, which lies on the safe side of the design. Section is designed for 90% of the load bearing capacity usage. Stirrups are taken regarding to structural requirements as $\phi 8$ loops spaced at 30 cm in the middle part of the column and 15 cm at base and head regions.

Table 1. Input data for column static design.

Column height	$H = 6.0$ m
Static load	$N_{Ed} = 1500$ kN
Bending moment	$M_{x,Ed} = 240$ kNm
	$M_{y,Ed} = 150$ kNm
Resultant load eccentricity	$e = 0.18868$ m
Steel class	S235
Concrete class	C20/25
Reinforcing steel class	BS500
Reinforcement cover	$c = 35$ mm
Required reinforcement ratio	$\rho_s = 2\%$

7. FEM NUMERICAL MODEL

Composite column which is the subject of the analyzes consists of three different materials: structural steel, concrete and reinforcing steel. Thus each has to be defined using proper finite element type and material properties to ensure most accurate simulation of the member behavior. Circular hollow section is modeled by S4R shell elements (Abaqus elements library) with four nodes and one Gauss integration point at the center of the element. For concrete C3D8R elements (Abaqus elements library) are used. It has eight-node cubic element with reduced Gauss integration at one point in the center of the element. In the Drucker-Prager material plasticity model it has to be chosen whether damage occurs due to exceeding the tension or compression stress limit. Tension criterion is defined herein, as for concrete tensile strength is much smaller, hence it is expected that damage will occur due to excessive tensile stresses. Longitudinal rebars and stirrups are modeled in Abaqus [6] using B31 beam elements with two nodes. Reinforcement is initially fully embedded in concrete, thus truss elements, i.e. T3D2 would be accurate enough for analysis. However, it is expected, that during blast situation, some parts of the reinforcement after concrete damage will be exposed and hence, bending stiffness definition (included in B31 type) of a rebar might be necessary.

Since the column is composite, proper interaction formulation is necessary. Two contact problems take place in the considered member. First is surface-to-surface contact between steel hollow section internal surface and concrete core external surface. This contact formulation is based on finite-sliding algorithm and the "hard" contact pressure-overclosure relationship [12]. Second is contact between reinforcement and concrete, which is encasing rebars and stirrups. Such contact definitions are most accurate, however the increase of computation time is significant.

Boundary conditions are simplified to the conventional approach. The base is a fixed connection as rigid joint with foundation pad, which is the most common engineering solution. Head of the column is pinned imitating joint with roof girders. It is reasonable to agree to such simplification, since the main purpose of this work is investigation composite column behavior under explosion situation. Introducing the phenomenon of joint flexibility would vastly complicate the whole problem formulation and eventually distort the results.

The analyzes conducted on numerical models of the column consist of two steps. First is static analysis applying boundary conditions, external static load and gravity to the body, in order to obtain static stress distribution. This is performed only once for each model, as it simulates the column state during its usual exploitation as a structure member. Second step is dynamic analysis in which static force and gravity is still applied to the column, however the

Table 2. Material parameters for numerical model.

		Section steel		Concrete		Reinforcement	
Mass density	[kg/m^3]	7860		2400		7860	
Isotropic Elasticity							
Young's modulus	[GPa]	310		30		210	
Poisson's ratio	[–]	0.3		0.2		0.3	
Isotropic plastic hardening H-M-H							
Yield stress	[MPa]	230	450	–		500	550
Plastic strain	[–]	0.00	0.25	–		0.00	0.25
Isotropic plastic hardening Drucker-Prager							
Angle of friction ϕ	[°]	–		65		–	
Flow stress ratio K	[–]	–		0.8		–	
Dilation angle ψ	[°]	–		45		–	
Strain rate dependence Power Law							
M	[1/s]	40		10		40	
n	[–]	5.0		3.5		5.0	
Ductile damage							
Fracture strain	[–]	10^{-1}	10^{-2}	10^{-2}	10^{-3}	10^{-1}	10^{-2}
Stress triaxiality	[–]	0.0	0.0	0.0	0.0	0.0	0.0
Strain rate	[1/s]	10^{-4}	10^{4}	10^{-4}	10^{4}	10^{-4}	10^{4}
Damage evolution linear, displacement-type							
Displacement at failure	[m]	0.01		0.001		0.01	

main load is defined as an Incident Wave using CONWEP tool. This step was conducted repeatedly, importing as Predefined Field results from static step. Parameters that were variable were the charge distance to the column and charge mass given in TNT equivalent, in order to find the minimum value of TNT needed to cause column failure.

For the dynamic step the explicit central-difference time integration rule is used. The main advantage over the implicit integration is the fact, that there is no need for finding a solution for a set of simultaneous equations, hence it requires no iterations and no tangent stiffness matrix. The basic principle of explicit method is calculating displacement, velocity and acceleration of the next increment directly, basing on previous increment data. This results in relatively inexpensive computation of each increment. Such procedure is efficient for short-time events. In this investigation the period tested was 50 ms. However there exists one important drawback. The method is conditionally stable, which means, that the time increment has to be small enough to ensure convergence of the

solution. An approximation to the stability limit is often written as the smallest transit time of a dilatational wave across any of the elements in the mesh:

$$(7.1) \qquad \Delta t \approx \frac{L_{\min}}{c_d},$$

where $L_{\min}$ is the smallest element dimension in the mesh and c_d is the dilatational wave speed. This condition is often referred to as Courant-Friedrichs-Lewy (CFL) condition [4], which describes the necessary condition for convergence while solving certain partial differential equations numerically by the method of finite differences, which are commonly used in explicit algorithms.

8. RESULTS

8.1. Member failure criteria

Aim of the analyzes is to find TNT equivalent minimum value, for a particular designed column, which causes its failure. However, the term failure may be interpreted in different ways. Therefore, it needs to be established, what is the failure criterion. A few options are available: first is visual inspection of the damage and take an arbitrary call, whether the column is considered destroyed or not. Second approach is observation of energy existing in the column or control column head displacement. Hence, the following criteria are available:

- strain energy,
- internal energy,
- kinetic energy,
- damage dissipation energy,
- equivalent plastic strain,
- displacement of selected column points,
- visual inspection.

Analyzes showed, that the best parameters for describing member failure are column head vertical displacement, kinetic energy and damage dissipation energy. Damaged column is still subjected to gravity and the structure dead load. This causes further increase of displacements and velocity, which is directly connected with kinetic energy. For a member that endured the blast event, one can observe stabilization of the displacements on certain level. Moreover, the kinetic energy decreases leading to the conclusion, that the member tends to go back to its primary configuration. Analyzing the damage dissipation energy, it can be estimated, what amount of the total energy caused material fracture eliminating the most exhausted FEM elements.

Figures 7 and 8 below show comparison of undamaged and destroyed columns. Energy and displacement plots show clearly the characteristics mentioned above.
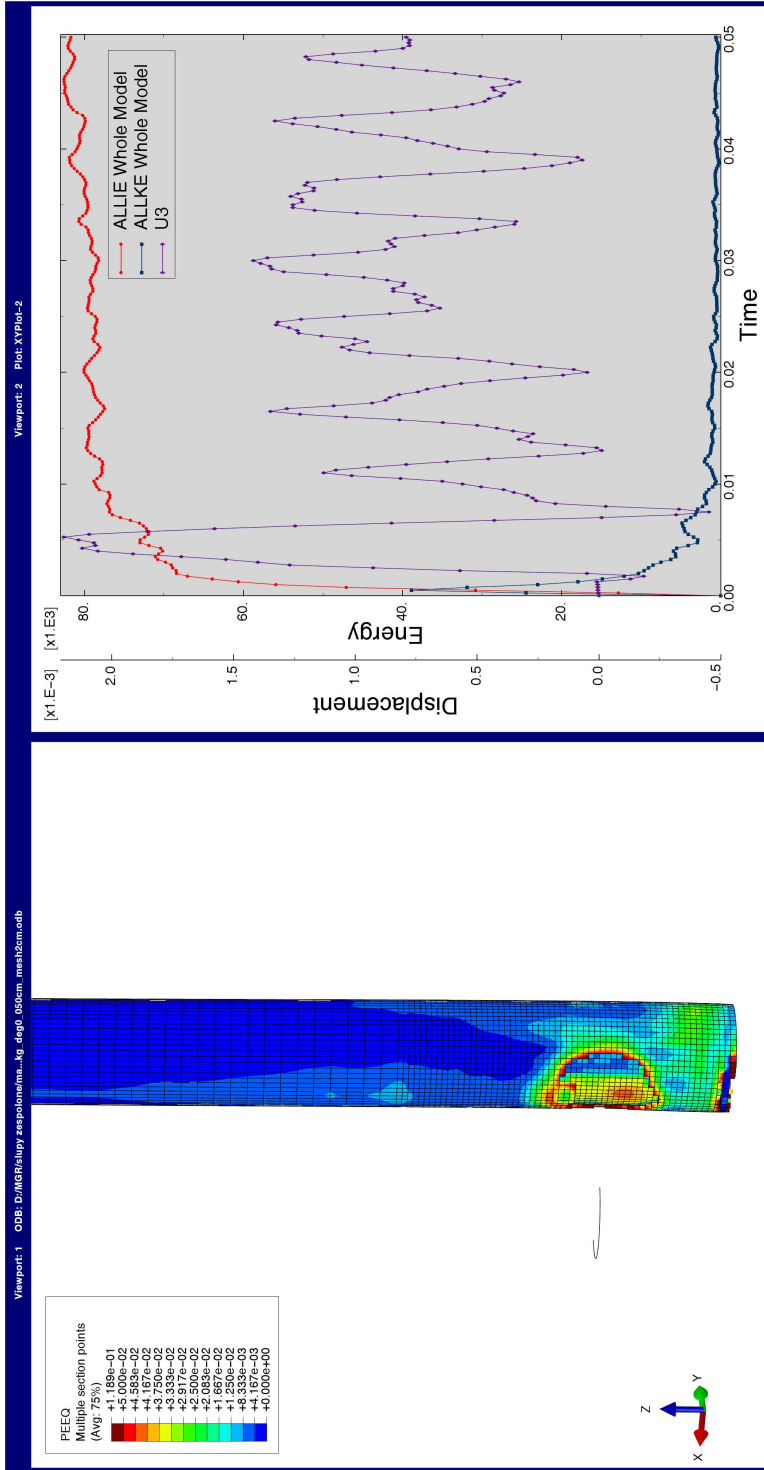
FIG. 7. Undamaged column – view without steel section, energy and displacement plot: (left) equivalent plastic strain at time 0.05 s, (right) model energies and column tip displacement curves.
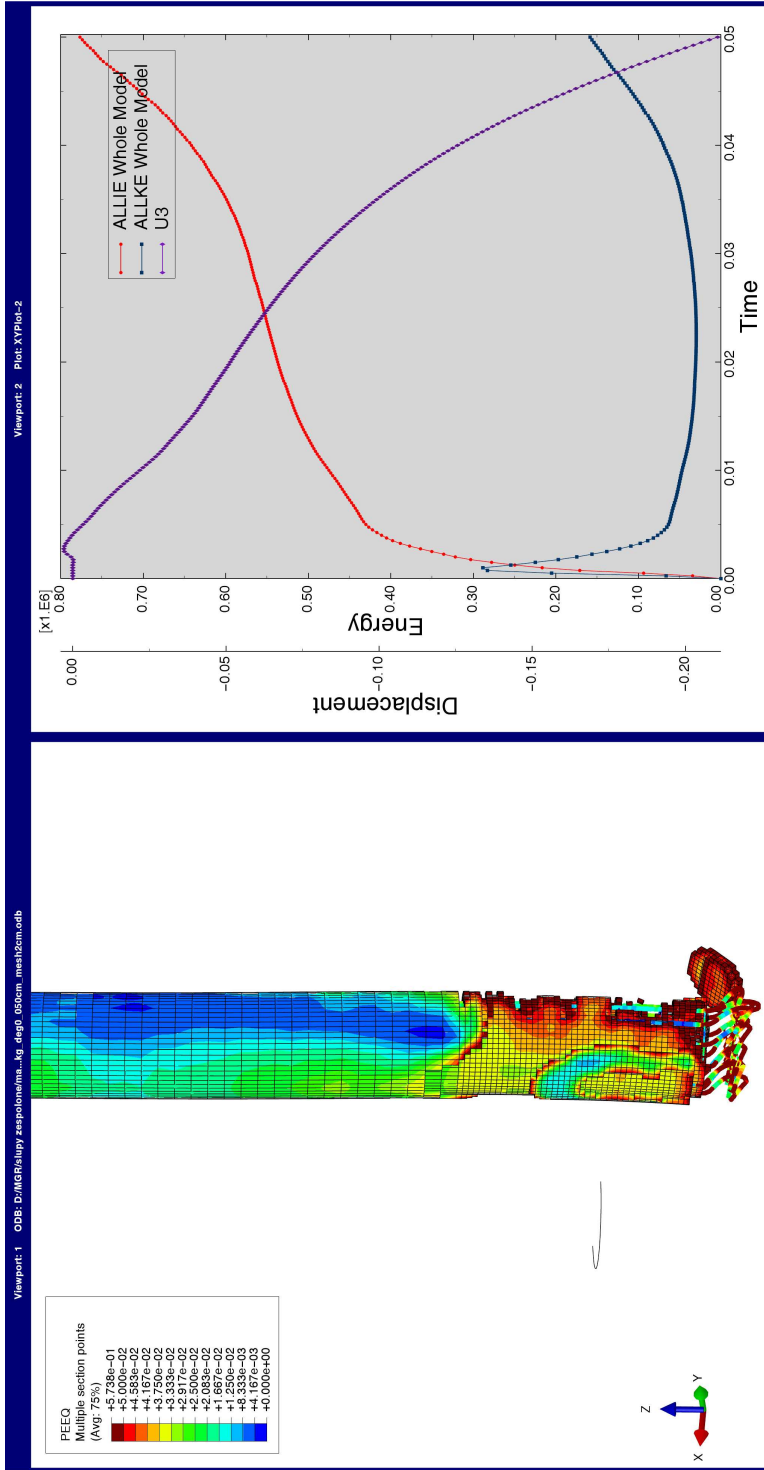
FIG. 8. Destroyed column – view without the steel section, energy and displacement plot: (left) equivalent plastic strain at time 0.05 s, (right) model energies and column tip displacement curves.

View of the steel section has been removed from these figures to visualize the state of the concrete core, in which damage is much more greater and occurs faster than in structural steel.

8.2. Reference column: results

The column designed as described before in chapter 6 was subjected to multiple analyzes with the TNT charge at three different distances: 0.5 m, 1.0 m and 2.0 m from the external surface of the column. The CONWEP model was set with properties modeling a surface blast, where the influence of blast wave reflection and self-amplification is taken into account. The charge was modeled at the level of 0.5 m above the column base, which is assumed to be the floor level in a building. Conducted analyzes present the least TNT mass of what would lead the member to failure according to criteria established before. Results printed in Table 3 show, that increasing the distance of charge placement, reduces immensely the destructive effects of blast event. The scaled distance parameter as per (1) proves, that the overpressure peak value of blast wave decreases as the wave travels, even though the influence of the medium flow is neglected in the analysis.

Table 3. Analysis results for the reference column.

Distance [m]	Charge mass [kg]	Scaled distance Z [m/kg$^{(1/3)}$]
0.5	27	0.1667
1.0	110	0.2087
1.5	227	0.2459
2.0	330	0.2894

The failure mechanism of investigated member presents interesting structure response. The most sharp and expressive effect is totally damaged slice of concrete core of approximately 15–20 cm width. This means, that for these particular concrete finite elements the excessive tensile stress was reached. After the local damage initiation, further strain increase leads to the damage evolution. Eventually, ultimate strain limit is reached, at which full material damage occurs. In that case the element is excluded from the analyzes, as it can no longer sustain or transfer any stresses. On the other hand, the external steel section, basing on visual inspection only, seems to be in good condition. Checking the equivalent plastic strain one can notice, that few elements have exceeded the value of 5%. This means, that probably the structural steel might serve still as a part of the building structure.

The explanation to such member behavior lies in the event nature. Abrupt overpressure peak applied to the external member surface induces sophisticated type of load. The pressure wave travels through the structure causing locally high internal stress of both signs in very short time. Moreover, the phenomenon of internal reflection appears on the connection between steel section and concrete core. Since the concrete core is of approximately seven times lower stiffness, the blast wave is reflected inwards repeatedly. Hence the concrete core having its tensile strength ten times lower than compressive strength yields first due to brittle fracture.

8.3. Strengthening solutions

The main aim of this work is to find solutions, how to increase the safety of the column during an explosion. Below are proposed a few options of improving composite column section strength in terms of resistance to blast load.

One of the ideas is to design the column assuming less usage ratio of load bearing capacity. It is based on the assumption, that stronger section in terms of static load resistance will be also more resistant to explosions. The static design was conducted again as described in Sec. 6 with the same input data, but with the usage parameter decreased by 30%. Table 4 presents output results for static

Table 4. Strengthened sections dimensions.
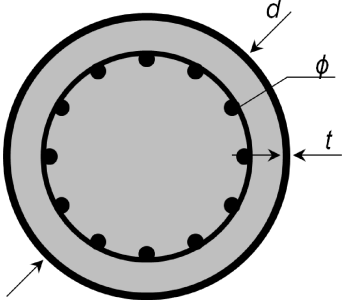
Case	Steel section diameter d [mm]	Steel section thickness t [mm]	Rebars number n [–]	Rebars diameter ϕ [mm]	Composite section factor δ [–]	Steel yield limit f_y [MPa]	Concrete tensile strength f_{ctk} [MPa]
Reference column	406.4	8.0	12	16	0.4835	235	3.0
60% load capacity used	508.0	6.0	8	25	0.3541	235	3.0
30% load capacity used	610.0	8.8	8	30	0.4030	235	3.0
Double pipe thickness 16 mm	406.4	16.0	12	16	0.6067	235	3.0
Higher steel class S355	406.4	8.0	12	16	0.5532	355	3.0
Higher concrete class C40/50	406.4	8.0	12	16	0.3579	235	4.6
Increase of reinforcement	406.4	8.0	12	25	0.4277	235	3.0

design with the load bearing capacity usage of 90%, 60%, 30% respectively and the further proposals described below.

Next proposals are based on improving particular elements of the section. First, very simple concept of thickening the steel section maintaining its design diameter. The thickness of 16 mm is twice as big as the original value. This solution might be easily implemented in practice as it involves only choosing thicker profile. Second, taking into the design higher steel grade – from S235 to S355 – results in increasing the steel yield stress limit by 50%. Next, increasing the concrete class from C20/25 to C40/C50 in general doubles its most important properties such as compressive and tensile strength. Also increase by 17% of the previous value in concrete stiffness modulus is observed. The solution is easy to implement, as it is not associated with any changes of dimensions of the member. The last but not least proposal is increasing of the longitudinal reinforcement. Conversion from 12ø16 to 12ø25 gives the effect of doubling the reinforcement ratio in this particular design. It is assumed that stronger reinforcement can overtake more destructive tensile stresses from the concrete core.

Results of analyzes performed on improved models are summarized in comparison with the reference column. Table 5 presents the increase in minimum charge mass value causing failure referring to the results from Table 4.

Table 5. Results summary.

Distance between column surface and charge position	Increase of minimum charge mass causing column failure			
	0.5 m	1.0 m	2.0 m	Average Δ_{TNT}
	[–]	[–]	[–]	[–]
Reference column	1.0000	1.0000	1.0000	**1.0000**
60% load capacity used	1.0000	0.9818	0.9091	**0.9636**
30% load capacity used	1.3333	1.4182	1.3333	**1.3616**
Double pipe thickness 16 mm	1.3333	1.5455	1.3152	**1.3980**
Higher steel class S355	1.0741	1.1091	1.1515	**1.1116**
Higher concrete class C40/50	1.0370	1.1273	1.1455	**1.1033**
Increase of reinforcement to 12ø25	1.1111	1.2727	1.1515	**1.1785**

The case of 60% load bearing capacity usage shows effect totally opposite to the desired result. Instead of growth, a decrease in minimum damaging charge mass is observed. The new section turns out to be more vulnerable than the reference one in terms of blast resistance. This proves the fact, that resistance to static loads is not directly related to dynamic load resistance. Although the section is thicker by 25%, the steel pipe thickness is smaller than in previous
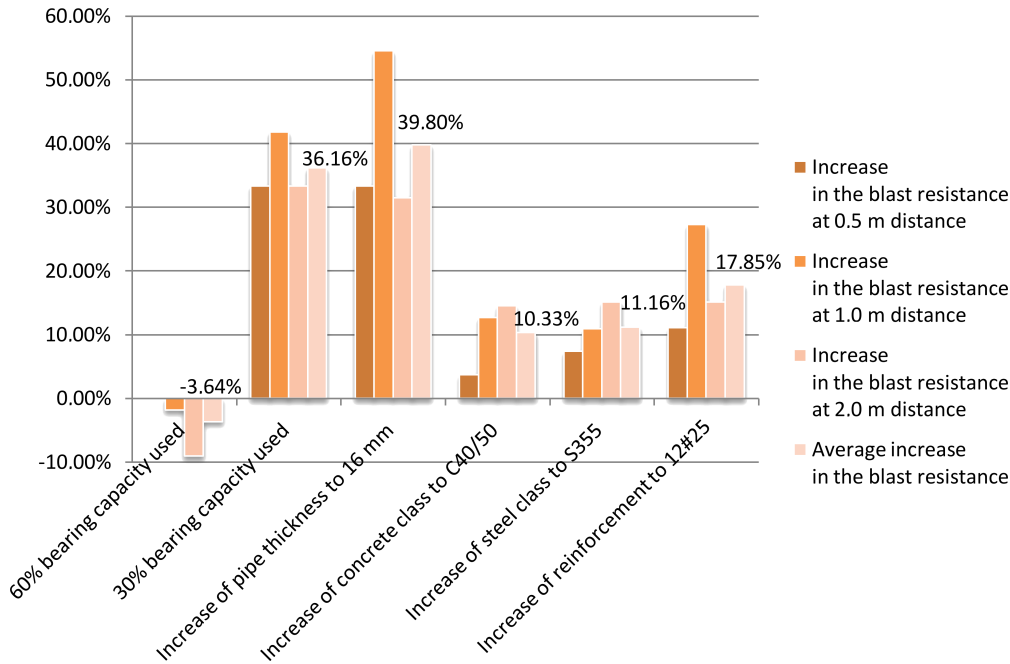
FIG. 9. Breakdown of blast resistance increase for different strengthening solutions.

configuration by 2 mm. This might be explanation for poorer performance during blast event. Steel can endure more severe dynamic actions due to its ductile properties. On the other hand, concrete is a brittle material. Therefore, introducing more concrete to the section does not improve blast resistance. Designing a case with 30% load capacity usage introduces significant increase in explosion resistance, however member dimensions grow severely, what causes too big expenses for the structure. Moreover, such big column diameter enlarge interferes with architectural concept of a building, which can disqualify the solution as well.

After doubling the steel profile thickness nearly 40% in average of blast resistance increase is a promising result, therefore this solution may be seriously taken into account in practice. The only drawback is twice as big the structural steel mass and hence, the cost of member production grows significantly. The case of introducing higher steel grade brings results, which are not very satisfactory, as 11.16% in average is not very significant growth. The section with higher concrete class, is not very advantageous for the member in terms of blast resistance. This proves again, that concrete is the weakest component of the member. Introducing double reinforcement ratio replacing the 12ø16 with 12ø25 returned results showing that this concept is justified to be used in practice.

It was expected, that strength results would occur proportional to the value of the distance of the charge ignition. Instead, the relative increases expressed in % in Table 4 indicate lack of such relation. However, Table 3 presents linear relation between the Scaled distance Z parameter for each case. This leads to the conclusion, that the Z value enables comparing blast effects more objectively than simple minimum charge mass value or simple relative increases expressed in percentages.

Furthermore, the value of minimum charge mass causing the member failure is not a sufficient parameter for comparing different members due to economical reasons. For example, the case of design with 30% load capacity used significantly enlarges mass of the member and such drawback needs to be properly accounted for. The idea is to merge the advantage of higher blast resistance and the disadvantage of higher concrete or steel mass (8.3, 8.3) into one coefficient defined herein as the blast strengthen efficiency parameter given in equation below:

$$（8.1） \qquad \eta \;=\; \frac{\Delta_{TNT}}{\Delta_E},$$

$$（8.2） \qquad \Delta_E \;=\; \frac{P^{(i)}}{P^{ref}},$$

$$（8.3） \qquad P^{(i)} \;=\; M_s^{(i)} P_{u,s}^{(i)} + V_c^{(i)} P_{u,c}^{(i)} + M_r^{(i)} P_{u,r}^{(i)},$$

where Δ_{TNT} is the relative charge mass increase and Δ_E is the column material price increase comparing to the reference member price. It is calculated using average unit prices in Poland of steel, concrete and reinforcement $P_{u,s}^{(i)}$, $P_{u,c}^{(i)}$, $P_{u,r}^{(i)}$ from the fourth quarter of 2012, gathered in pricing books the "Sekocenbud" series.

The strengthening efficiency factor η values reveal the correlation between increasing member blast resistance and the drawbacks of increasing its dimensions. Higher material costs of improved members present the impact of the economical circumstances on the investigated problem. Nevertheless, due to variability of prices caused by criteria such as location, transportation, etc., it has been simplified to the shape in Eq. (8.1).

Table 6 shows clearly the drawbacks of enlarging the column in the concept of higher static load capacity. The case of 30% member returned the second highest resistance increase of 36.16%. However, the steel and concrete usage would consume the benefits of implementing this solution, which makes it inefficient. On the other hand, the case of higher steel class seems to be the most reasonable solution, though as it has been mentioned before, exact material prices may vary according to specific location etc.

Table 6. Strengthening efficiency factor for proposed members.

Case	Estimated column price	Relative price increase	Charge mass increase	Strengthening efficiency factor
	P [EUR]	Δ_E [–]	Δ_{TNT} [–]	η [–]
Reference column	466.01	1.0000	1.0000	**1.0000**
60% load capacity	567.62	1.2180	0.9636	**0.7911**
30% load capacity	899.24	1.9296	1.3616	**0.7056**
Double pipe thickness	728.27	1.5628	1.3980	**0.8946**
Higher steel class	477.48	1.0246	1.1116	**1.0849**
Higher concrete class	490.73	1.0530	1.1033	**1.0477**
Increase of reinforcement	667.48	1.4323	1.1785	**0.8228**

9. Conclusions

Although military facilities, skyscrapers, nuclear power plants and dams are designed to resist explosive loads, the majority of public buildings is vulnerable to terrorist attacks, least because of lack of estimation of explosion situation effects. Even a small amount of charge placed in critical point can cause very serious damage. There exists a need to provide solutions how to protect structures against blasts, both, newly designed objects, as well as improve the safety of already existing ones.

The column failure mechanism occurs to be fairly complex. It is not possible to choose one criterion to determine whether the member is considered destroyed or not. It is a combination of different energy types in the material, its velocity, displacement and expected equilibrium state. Especially in the case of composite columns there exists the threat of underestimating the damage. Even though steel section may look stable, the concrete core may be subjected to large fracture.

Among the proposed strengthening solutions the concepts of increasing static load capacity turned out to be unsuccessful. Economical drawbacks of these changes consume the benefits in blast resistance. Analyzes lead to the conclusion, that the most promising ideas are connected with improving the steel section performance, both increasing its thickness and the limit yield stress gave good results.

As a final remark it may be noted, that more attention to explosion load has to be brought during the design procedure of buildings. Design codes used in Europe mention about taking into consideration possible explosions during load collecting and instructs to treat it as an accidental situation. However, it does

not provide the user with any guidance how to estimate and model the effects of a blast event. This raises the need to address this deficiency.

References

1. BAZANT Z.P., *Concrete fracture models: Testing and practice*, Engineering Fracture Mechanics, **69**, 165–205, 2001.

2. BISCHOFF P.H., PERRY S.H., *Compressive behaviour of concrete at high strain rates*, Materials and Structures, **24**, 425–450, 1991.

3. CHOCK J.M.K., KAPANIA R.K., *Review of two methods for calculating explosive air blast*, Shock and Vibration Digest, **33**, 91–102, 2001.

4. COURANT R., FRIEDRICHS K., LEWY H., *On the partial difference equations of mathematical physics*, IBM Journal of Research and Development, **11**, 215–234, 1967.

5. COWPER G.R., SYMOND P.S., *Strain Hardening and Strain Rate Effects in the Impact Loading of Cantilever Beams*, Applied Mathematics Report No. 28, Brown University, Providence, Rhode Island, USA, 1957.

6. Dassault Systemes, Abaqus 6.11 Documentation, 2011.

7. DRUCKER D.C., PRAGER W., *Soil mechanics and plastic analysis or limit design*, Quart. Appl. Math., **10**, 157–165, 1952.

8. GAJEWSKI T., GARBOWSKI T., *Calibration of concrete parameters based on digital image correlation and inverse analysis*, Archives of Civil and Mechanical Engineering, **14**, 1, 170–180, 2014.

9. GAJEWSKI T., GARBOWSKI T., *Mixed experimental/numerical methods applied for concrete parameters estimation*, Proceedings of XX International Conference on Computer Methods in Mechanics CMM2013, Recent Advances in Computational Mechanics, T. Łodygowski, J. Rakowski, P. Litewka [Eds.], 293–302, CRC Press, 2014.

10. GARBOWSKI T., MAIER G., NOVATI G., *Diagnosis of concrete dams by flat-jack tests and inverse analyses based on proper orthogonal decomposition*, Journal of Mechanics of Materials and Structures, **6**, 1–4, 181–202, 2011.

11. GEORGIN J.F., REYNOUARD J.M., *Modeling of structures subjected to impact: Concrete behaviour under high strain rate*, Cement and Concrete Composites, **25**, 131–143, 2003.

12. GOYAL S., PINSON E.N., SINDEN F.W., *Simulation of dynamics of interacting rigid bodies including friction I: General problem and contact model*, Engineering with Computers, **10**, 162–174, 1994.

13. GURSON A.L., *Continuum Theory of Ductile Rupture by Void Nucleation and Growth: Part I – Yield Criteria and Flow Rules for Porous Ductile Materials*, Journal of Engineering Materials and Technology, 99, 2–15, 1997.

14. HERV G., GATUINGT, F., IBRAHIMBEGOVI A., *On numerical implementation of a coupled rate dependent damage-plasticity constitutive model for concrete in application to high-rate dynamics*, Engineering Computations (Swansea, Wales), **22**, 583–604, 2005.

15. HILLERBORG A., MODEER M., PETERSSON P.E., *Analysis of Crack Formation and Crack Growth in Concrete by Means of Fracture Mechanics and Finite Elements*, Cement and Concrete Research, **6**, 773–782, 1976.

16. Huntington-Thresher W., Cullis I.G., *TNT blast scaling for small charges*, Proceedings of 19th Int. Sym. on Ballistics, Interlaken, Switzerland, 647–654, 2001.

17. Kingery C.N., Bulmash G., *Airblast parameters from TNT spherical air burst and hemispherical surface burst*. Technical Report ARBRL-TR-02555, U.S. Army Ballistic Research Laboratory, 1984.

18. Lee J., Fenves G.L., *Plastic-damage model for cyclic loading of concrete structures*, Journal of Engineering Mechanics, **124**, 892–900, 1998.

19. Lubliner J., Oliver J., Oller S., Oate E., *A plastic-damage model for concrete*, International Journal of Solids and Structures, **25**, 299–326, 1989.

20. Zirpoi A., Novati G., Maier G., Garbowski T., *Dilatometric tests combined with computer simulations and parameter identification for in-depth diagnostic analysis of concrete dams*, Proceedings of the International Symposium on Life-Cycle Civil Engineering IALCCE '08, CRC Press, 259–264, 2008.

21. McAllister T.P., Gross J.L., Sadek F., Kirkpatrick S., MacNeill R.A., Zarghamee M., Erbay O.O., Sarawit A.T., *Analysis of structural response of WTC 7 to fire and sequential failures leading to collapse*, Journal of Structural Engineering, **138**, 1, 109–117, 2012.

22. Neuberger A., Peles S., Rittel D., *Scaling the response of circular plates subjected to large and close-range spherical explosions. Part II: Buried charges*, International Journal of Impact Engineering, **34**, 874–882, 2007.

23. Ngo T., Mendis P., Gupta A., Ramsay J., *Blast loading and blast effects on structures – An overview*, Electronic Journal of Structural Engineering, **7**, 76–91, 2007.

24. Rodriguez-Nikl T., Lee C.-S., Hegemier G.A., Seible F., *Experimental performance of concrete columns with composite jackets under blast loading*, Journal of Structural Engineering, **138**, 1, 81–89, 2012.

25. Ross C. Allen, Thompson P.Y., Tedesco J.W., *Split-Hopkinson pressure-bar tests on concrete and mortar in tension and compression*, ACI Materials Journal, **86**, 475–481, 1989.

26. Rule W.K., Jones S.E., *A Revised Form for the Johnson-Cook Strength Model*, International Journal of Impact Engineering, **21**, 609–624, 1989.

27. Soutis C., Mohamed G., Hodzic A., *Modelling the structural response of GLARE panels to blast load*, Composite Structures, **94**, 267–276, 2011.

28. The MathWorks, Inc., Matlab R2011a Documentation, 2011.